

COPY RIGHT



ELSEVIER
SSRN

2022 IJIEMR. Personal use of this material is permitted. Permission from IJIEMR must be obtained for all other uses, in any current or future media, including reprinting/republishing this material for advertising or promotional purposes, creating new collective works, for resale or redistribution to servers or lists, or reuse of any copyrighted component of this work in other works. No Reprint should be done to this paper, all copy right is authenticated to Paper Authors

IJIEMR Transactions, online available on 26th Dec 2022. Link

[:http://www.ijiemr.org/downloads.php?vol=Volume-11&issue=Issue 12](http://www.ijiemr.org/downloads.php?vol=Volume-11&issue=Issue 12)

10.48047/IJIEMR/V11/ISSUE 12/143

TITLE: A STUDY OF X-RAYS BINARIES POTENTIAL OF SUPER SOFT X-RAYS BINARIES SOURCES

Volume 11, ISSUE 12, Pages: 1068-1077

Paper Authors **Angira Brahma, Dr. Veeresh Kumar**



USE THIS BARCODE TO ACCESS YOUR ONLINE PAPER

To Secure Your Paper As Per **UGC Guidelines** We Are Providing A Electronic Bar Code

A STUDY OF X-RAYS BINARIES POTENTIAL OF SUPER SOFT X-RAYS BINARIES SOURCES

Candidate name- Angira Brahma

Designation- research scholar sunrise university alwar

Guide name- Dr. Veeresh Kumar

Designation- Assistant Professor sunrise university alwar

ABSTRACT

The variability studies have revealed an assortment of phenomena within X-ray point sources, ranging from periodic and quasi-periodic variability associated with binary systems to irregular fluctuations associated with accretion processes. The understanding of X-ray binaries, active galactic nuclei, and intermediate-mass black holes has significantly benefited from these investigations, providing valuable clues about their mass, accretion rates, and intrinsic properties. Furthermore, we explore the potential correlations between X-ray point source variability and various galactic properties, such as the host galaxy's age, stellar mass, and metallicity. Such relationships can help constrain the underlying physical mechanisms governing X-ray emission and accretion processes within these elliptical environments. The abstract also highlights the importance of future X-ray missions in expanding our understanding of X-ray point source variability in elliptical galaxies. The upcoming generation of X-ray observatories with enhanced capabilities is expected to provide deeper insights into the most energetic and transient events occurring in these galactic systems.

KEYWORDS: X-Rays Binaries Potential, Super Soft, phenomena, accretion processes, X-ray observatories

INTRODUCTION

The SD channel is supported by the expected outputs of the merger of two white dwarfs, O+Ne+Mg by off-center carbon ignition and neutron star via accretion-induced collapse (AIC), while the AIC channel is discouraged by the symmetry of the SN Ia explosion and the lack of companion stars observed after the SN Ia, i.e. near the location of the supernova remnant (hereafter SNR). Supernovae are represented worldwide in Figure 1, which is a categorization diagram. The study of binary systems containing a white dwarf (WD) as the primary component and either a massive star (MS; this case is known as symbiotic) or a red giant (RG; this case also leads to cataclysmic variations; for example, recurrent novae or dwarf novae) that is accreting onto the WD is, therefore, apparently necessary for an understanding of the SD channel. Beginning in the 1970s with pioneer (computationally speaking) works like Paczynski's (1970), accreting binary systems have been an excellent source of research.

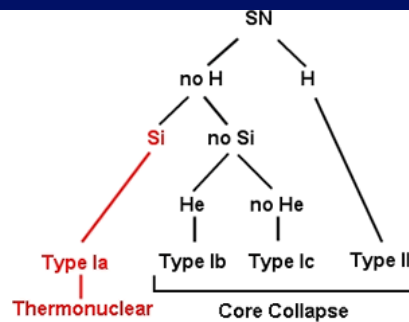


Figure 1 Scheme of types of SNe: SN Type Ia contains no hydrogen but silicon lines; it is thought to be the product of thermonuclear explosions of white dwarfs. Core-collapse SNe are the result of explosions of massive stars; in general, there are different type of these events depending on the absence of the certain elements on the spectra: Type Ib contains no hydrogen, no silicon but helium lines, while Type Ic lacks the same elements as Type Ib plus helium; if SNe contains hydrogen it is catalogued as Type II (even though there are differences depending on their light curves). From COSMOS webpage.

which describes the evolution of close binaries: given a range of values for the periods, initial masses, and distances between the stars (which are not independent but related by the third Kepler law), mass transfer (hereafter MT) is expected to arise, for instance whenever the stellar radius of the donor exceeds a critical radius, defined approximately as the radius of its Roche lobe, through the inner Lagrangian point L1.

For instance, if the primary, the more massive star initially, fills several times its Roche lobe and MTs occur during its evolution to a WD, accreting matter to the -ultimately more massive- secondary star, which ends up filling its own Roche lobe and transferring mass to the WD, one can easily imagine how a WD + MS/RG system may be formed during the transition from the main sequence to the red giant branch, where the radius of a 1

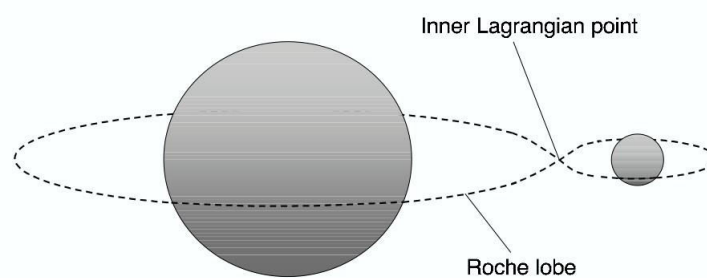


Figure 2 Scheme of a binary stars system with their respective Roche Lobes (equipotential surface surrounding each star), and the inner Lagrangian point L1 (the intersection of the Roche Lobes in the equatorial plane). From Iliadis (2007).

Binary stellar evolution of a WD + (non-degenerated) star system has traditionally been studied by placing an already-evolved WD + donor at the beginning of MT using a grid of three-parameters (M_{wd} , M_{donor} , and P_{orb}) shown in Figure 3, then following a detailed stellar structure time evolution of the binary, including the model of accretion, and distinguishing as a progenitor tho The number of CO WD + MS systems, for instance, at a certain star formation rate (SFR) or after a single outburst, was then calculated using quick

binary population synthesis (BPS) calculations. The binary evolution from ZAMS has been followed by a number of recently developed BPS codes, with modifications to the CE-prescription, mass retention efficiencies, angular momentum losses by RLOF, etc.

Since the normal maximum initial WD mass is considered to be $1.2M_{\odot}$, and the lowest starting mass determined for a successful progenitor WD of an SN Ia is $0.65M_{\odot}$ (for $Z = 0.02$), the WD needs to accrete at least $0.2M_{\odot}$ in the SD channel in order to ignite. Over-luminous SN Ia events like SNLS-03D3B may be explained by factors including rotation that augment the WD mass at ignition. The brightness

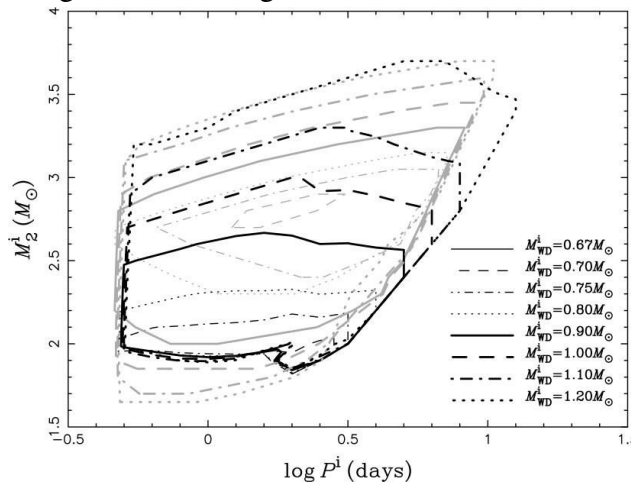


Figure 3 Initial parameters in the Mdonor –Porb for different WD masses (0.7 to 1.2M_⊙) (inner to outer region) of all progenitors of SN Ia. From Han & Podsiadlowski (2004).

(2.2 LSNIa) and kinetic energy calculated from this SN's spectral lines pointed to a WD explosive mass greater than M_{ch} . Once the WD reaches this mass, the brightness, color, and spectral feature development of "normal" SN Ia agrees with explosion theories (delayed detonation, carbon deflagration, off-center carbon igniting).

TIME-DEPENDENT PERTURBATIONS

The second objective of this chapter is to determine how level transitions occur in order to comprehend the so-called banned transitions once the first formulation has been established. While the standard examples of time-independent Hamiltonians and degenerate perturbation of states are ignored, it is important to note that from this point on, LS coupling will be assumed, meaning that the spin-orbit interaction's ($\propto L \cdot S$) contribution to the Hamiltonian will be seen as a perturbation. Since L^2 and S^2 operators commute with H , we may extrapolate that the total angular momentum J^2 and its projection in, say, the zaxis J_z are likewise good operators, where good is defined as

$$\begin{aligned} \hat{J} &\equiv \hat{L} + \hat{S} \\ \rightarrow \hat{J}^2 |j, m_j\rangle &= j(j+1)\hbar^2 |j, m_j\rangle \\ \rightarrow \hat{J}_z |j, m_j\rangle &= m_j \hbar |j, m_j\rangle. \end{aligned}$$

In accordance with the time-dependent perturbation theory, we modify the classical time-

independent quantum Hamiltonian (H0) by adding a minor time-dependent perturbation (H1)

so that $H_0|i\rangle = E_i|i\rangle$.

$$H = H_0 + H_1(t).$$

For $H(t) = H$, Operator 2.6 in Time Gives Way to

$$T(t, t_0) = \exp \left\{ -\frac{iH(t - t_0)}{\hbar} \right\}.$$

The temporal evolution of a universal ket $|A\rangle$ (Equation), starting at time $t = t_0$, and the probability $P_f(t)$ to "jump" to the state $|f\rangle$, in the absence of disturbance, are expressed as

$$\begin{aligned} |A, t_0, t\rangle &= \sum_i c_i T(t, t_0) |i\rangle \\ P_f(t) &\equiv |\langle f|A, t, t_0\rangle|^2 \\ &\rightarrow = \left| \sum_i c_i \exp \left\{ -\frac{iE_i(t - t_0)}{\hbar} \right\} \underbrace{\langle f|i\rangle}_{\delta_{fi}} \right|^2 \\ &\rightarrow = |c_f|^2 \\ &\Rightarrow P_f(t) = P_f(t_0) \end{aligned}$$

That is to say, P_f is constant, and not subject to change. The coefficients c_i in Equation change as a function of time for a time-dependent Hamiltonian.

$$|A, t_0, t\rangle = \sum_i c_i(t) \exp \left\{ -\frac{iE_i(t - t_0)}{\hbar} \right\} |i\rangle.$$

$H = H_0 + H_1$ and $RHS = LHS$ in the time-dependent Schrödinger equation (Equation).

$$\text{RHS: } \langle f|(H_0 + H_1)|A, t_0, t\rangle = \langle f| \sum_i c_i(t) \exp \left\{ -\frac{E_i(t - t_0)}{\hbar} \right\} (E_i + H_1)|i\rangle$$

$$\rightarrow = \underbrace{\sum_i c_i(t) \exp \left\{ -\frac{E_i(t - t_0)}{\hbar} \right\}}_{c_f(t) E_f \exp \left\{ -\frac{iE_f(t - t_0)}{\hbar} \right\}} \left(E_i \overbrace{\langle f|i\rangle}^{\delta_{fi}} + \langle f|H_1|i\rangle \right)$$

$$\text{LHS: } \langle f|i\hbar \frac{\partial}{\partial t} (|A, t_0, t\rangle) = \sum_i \left[i\hbar \frac{dc_i(t)}{dt} + c_i(t) E_i \right] \exp \left\{ -\frac{iE_i(t - t_0)}{\hbar} \right\} \overbrace{\langle f|i\rangle}^{\delta_{fi}}$$

$$\rightarrow = \left(i\hbar \frac{dc_f(t)}{dt} + c_f(t) E_f \right) \exp \left\{ -\frac{iE_f(t - t_0)}{\hbar} \right\}$$

$$\Rightarrow i\hbar \frac{dc_f(t)}{dt} = \sum_i H_{fi}(t) \exp \{ i\omega_{fi}(t - t_0) \} c_i(t)$$

With

$$H_{fi} = \langle f | H_1(t) | i \rangle$$

$$\omega_{fi} = \frac{E_f - E_i}{\hbar}$$

It is now evident that the likelihood of moving from state i to state f will fluctuate according to the time-varying coefficients $c_f(t)$, as shown by the equation.

1.2.1 Dyson Series

The answer to Equation is required to resume the analysis begun in Equation. The quickest and easiest method is establishing a "new" time evolution operator of the

$$T(t_0, t) = \exp \left\{ \frac{-iH_0(t - t_0)}{\hbar} \right\} T_I(t_0, t)$$

conditional on $T(t_0, t_0) = 1$. It is straightforward to demonstrate that $T_I(t, t_0)$ satisfies Equation 2.5 if we substitute for $H = H_0 + H_1$.

$$i\hbar \frac{\partial T_I(t_0, t)}{\partial t} = H_I(t_0, t) T_I(t_0, t)$$

using the formula $H_I(t_0, t) = \exp(iH_0(t-t_0)) H_1 \exp(-iH_0(t-t_0))$. All of the state change data is stored in H_I . The transition probability $P_{if} = |c_f(t)|^2$ and the transition probability $c_f(t)$ may be expressed in terms of $T_I(t_0, t)$ if the system is characterized by $|i\rangle$ at t_0 and transitions to state $|f\rangle$ at time t .

$$\begin{cases} 2.22 \rightarrow \langle f | i, t_0, t \rangle = c_f(t) \exp \left\{ \frac{-iE_f(t-t_0)}{\hbar} \right\} \\ 2.4 \rightarrow \langle f | i, t_0, t \rangle = \exp \left\{ \frac{-iE_f(t-t_0)}{\hbar} \right\} \langle f | T_I(t_0, t) | i \rangle \end{cases}$$

$$\Rightarrow c_f(t) = \langle f | T_I(t_0, t) | i \rangle$$

$$\Rightarrow P_{i \rightarrow f}(t_0, t) = |\langle f | T_I(t_0, t) | i \rangle|^2$$

Finding the operator $T_I(t_0, t)$ yields an explicit equation for Eqs. 2.29 and 2.30. The Dyson series provides a close approximation to this problem's solution:

$$T_I(t_0, t) \simeq 1 + \left(\frac{-i}{\hbar} \right) \int_{t_0}^t dt' H_I(t_0, t') + \left(\frac{-i}{\hbar} \right)^2 \int_{t_0}^t dt' \int_{t_0}^{t'} dt'' H_I(t_0, t') H_I(t_0, t'') \dots$$

Finally, the probability is established by substituting Equations for the first two coefficients in the formula $c_f(t) = c_f(t-1) + c_f(t-2)$.

$$\begin{cases} c_f^{(0)} = \delta_{if} \\ c_f^{(1)} = \left(\frac{-i}{\hbar} \right) \int_{t_0}^t dt' \exp \{ i\omega_{fi} \} H_{fi}(t') \\ \vdots \end{cases}$$

$$\Rightarrow P_{i \rightarrow f}(t_0, t) = |c_f^{(0)} + c_f^{(1)} + c_f^{(2)} + \dots|^2$$

The next step is to use the computed probability of the transition to calculate the transition

rate, given the beginning and end states.

Fermi's Golden Rule

The precise pace of transition between states is what Fermi's golden rule reveals. The term "transition rate" has been defined as

$$w_{i \rightarrow [f]}(t) = \frac{dP_{i \rightarrow [f]}(t)}{dt}$$

Let's suppose a rapid change to H_0 of the type $H_1(t \geq 0) = H_1$ in order to derive the rule. For the sake of brevity, suppose H_1 is temporally invariant. The coefficients in 2.32 are calculated by utilizing the definitions in Equations 2.24 and 2.25 to get $P_{if}(t)$, where only the $c_f^{(1)}(t)$ coefficient is used. This leads to the formula $P_{if}(t) = |c_f^{(1)}(t)|^2$ for the probability, and

$$c_f^{(1)}(t) = \frac{H_{fi}}{E_f - E_i} [1 - \exp(i\omega_{fi}t)]$$

$$P_{i \rightarrow [f]} = \frac{4 |H_{fi}|^2}{|E_f - E_i|^2} \sin^2 \left\{ \frac{(E_f - E_i)t}{2\hbar} \right\}$$

Transitions that result in an energy balance, $E_f = E_i$, will be prioritized. There is a set of (final) states that have almost the same energy as E_i , hence care must be used while transitioning from state $|i\rangle$. This occurs across a density of states ($\rho(E_f)$). This is reflected in the definition of the joint probability over these states as

$$P_{i \rightarrow [f]}(t) = \int_{-\infty}^{\infty} dE_f P_{i \rightarrow f}(t) \rho(E_f)$$

The true probability and thus the transition rate 2.34 is obtained by substituting 2.35 into the previous equation and noting that P_{if} is only non-zero at $E_f = E_i$, where $\rho(E_f)$ and $|H_{fi}|^2$ are practically constant.

$$P_{i \rightarrow [f]}(t) = \frac{2\pi}{\hbar} |H_{fi}|^2 \rho(E_f) t \Big|_{E_f \approx E_i}$$

$$\Rightarrow w_{i \rightarrow [f]} = \frac{2\pi}{\hbar} |H_{fi}|^2 \rho(E_f) \Big|_{E_f \approx E_i}$$

$$\equiv \frac{2\pi}{\hbar} |H_{fi}|^2 \delta(E_f - E_i)$$

The equation has a more common name: "Fermi's Golden Rule"¹². Using this principle on the Hamiltonian $H_1(t)$ for harmonic perturbations,

$$H_1(t) = V \exp(i\omega t) + V^\dagger \exp(-i\omega t)$$

the coefficient $c_f^{(1)}(t)$ in the second part of Equation 2.32 is found by doing the following:

$$c_f^{(1)}(t) = \frac{1}{\hbar} \left(\frac{1 - \exp \{i(\omega_{fi} + \omega)t\}}{\omega_{fi} + \omega} V_{fi} + \frac{1 - \exp \{i(\omega_{fi} - \omega)t\}}{\omega_{fi} - \omega} V_{fi}^\dagger \right)$$

In this case $V_{fi} = f |V| |i\rangle$ and $V_{fi} = f |V| |i\rangle$. When considering the exponentials, we find two situations where $P(t) = c_f(t)$ does not vanish at $t \rightarrow \infty$:

$$\begin{aligned} \omega_{fi} + \omega > 0 & \quad \text{or} \quad E_f - E_i - k\omega \\ \omega_{fi} - \omega > 0 & \quad \text{or} \quad E_f - E_i + k\omega \end{aligned}$$

Clearly, in instance 2.42, E_f will have less energy than E_i by a factor of k , resulting in a net loss of energy to the perturbing field. instance 2.43 is the inverse of instance 2.42, with the system gaining energy. In the first scenario, it is called stimulated emission, whereas in the later one, it is called absorption.

Interaction e-EM Wave

From now on, you must think in terms of Local Thermodynamic Equilibrium (LTE): LTE is defined by Collins (1989), Chapter 1, as the (statistical) equilibrium of particles like free electrons, following the Maxwell-Boltzmann statistics (or Fermi-Dirac in case of degeneracy), and photons, following the Planck distribution¹³, both described by a single temperature T , as long as the mean free path of the particles that

All microscopic processes must be balanced by its inverse, a notion known in thermodynamics as "detailed balance" (Osterbrock & Ferland, 2006). In this sense, it implies that every time a photon is absorbed, it must be replaced by an equal and opposite emission. particular the interplay of the system with a particular (external) disturbance, it follows from the previous section that this concept must account for stimulated emission and absorption. However, this is just part of the picture; in quantum physics, there is a non-zero chance that an electron can spontaneously "jump" from energy level E_i to energy level E_f by emitting a photon without any external trigger.

To determine an explicit form of the absorption and emission coefficients, we use the Hamiltonian of the interaction between an electromagnetic (EM) wave and an electron and include this emission into the detailed balance equation for the transition. In the classical setting, the Coulomb potential is used to express H in terms of the vector potential $A(x)$ and the scalar potential $\Phi(x)$. $\nabla \cdot A = 0$:

$$\begin{aligned} H &= \frac{(\hat{p} + e\vec{A})^2}{2m_e} - e\phi + \underbrace{\Phi(x)}_{x \rightarrow r} \\ \Rightarrow H &= \underbrace{\frac{p^2}{2m_e} + \Phi(r)}_{H_0} + \underbrace{\frac{\vec{A} \cdot \hat{p}}{m_e} + \frac{e^2 A^2}{2m_e}}_{H_1} - e\phi \end{aligned}$$

Has a key potential of $\Phi(r)$. The phrase $\vec{A} \cdot \hat{p}$, which includes the EM-e interaction while ignoring the term A^2 , is used. A plane-wave with a certain angular frequency is the simplest solution to the wave equation. ω , polarization direction $\rightarrow \epsilon$, direction of propagation $\rightarrow n$ (hence $\epsilon \cdot n = 0$) and c the speed of light,

$$\varphi = 0$$

$$\vec{A}(\mathbf{x}, t) = 2A_0 \cos \left\{ \left(\frac{\omega}{c} \right) \vec{n} \cdot \mathbf{x} - \omega t \right\} \vec{e}$$

A great illustration of incident radiation. When the last equation in Equation 2.46 is substituted with the time-dependent Hamiltonian, we get

$$H_1 = \frac{eA_0}{m_e} \left[\exp \left\{ i \left(\frac{\omega}{c} \right) \vec{n} \cdot \mathbf{x} - i\omega t \right\} + \exp \left\{ -i \left(\frac{\omega}{c} \right) \vec{n} \cdot \mathbf{x} - i\omega t \right\} \right] \vec{e} \cdot \hat{p}$$

Taking a look at Fermi's golden rule for harmonic oscillations (Equation 2.40), it becomes apparent that if

$$V = \frac{eA_0}{m_e} \exp \left\{ -i \left(\frac{\omega}{c} \right) \vec{n} \cdot \mathbf{x} \right\} \vec{e} \cdot \hat{p}$$

rates of transition between absorption and stimulated emission are calculated using Equations First, define d_{fi} , which may be interpreted as the transition's multipole moment.

Electric and Magnetic Multipole transitions

Radiation of the correct wavelength induces the i_f and f_i transitions. λ

$$\lambda = \frac{2\pi c}{\omega} \sim 10^3 \text{ \AA} \sim 10^{-7} \text{ m}$$

Their distances from one another are around four orders of magnitude larger than the radius of a hydrogen atom, which is on the order of 1011 m. So, in theory, we may get a good approximation to the exponential in Eq. 2.49 if we do

$$\exp \left\{ i \left(\frac{\omega}{c} \right) \vec{n} \cdot \mathbf{x} \right\} = 1 + i \left(\frac{\omega}{c} \right) \vec{n} \cdot \mathbf{x} + \dots$$

Electric dipole approximation is found by using the first term of the formula. The elements of the dipole matrix are found by solving $[x, H_0] = ikp$.

By

$$\begin{aligned} \mathbf{d}_{if} &= \langle i | \mathbf{x} | f \rangle \\ \rightarrow \langle i | z | f \rangle &\neq 0 \quad \text{only if} \quad \Delta l = \pm 1, \Delta m = 0 \\ \rightarrow \langle i | y | f \rangle &\neq 0 \quad \text{only if} \quad \Delta l = \pm 1, \Delta m \pm 1 \\ \rightarrow \langle i | x | f \rangle &\neq 0 \quad \text{only if} \quad \Delta l = \pm 1, \Delta m \pm 1 \\ &\text{and} \\ \Delta m_s &= 0 \end{aligned}$$

utilizing the latter choice rule because the dipole matrix is spin16-independent. The principles for choosing an electric dipole are expressed in terms of the total angular momentum $j = |l\ s| \bullet \bullet 1 + s$ and the magnetic quantum number $m_j = j, j + 1, \dots, m_j 1, j$ (in LS coupling):

$$\Delta j = 0, \pm 1$$

$$\Delta m_j = 0, \pm 1$$

Thus, owing to spherical symmetry, transitions to $j = 0$ are not allowed. Forbidden changes are those that cannot occur due to electric dipole selection. The elements of the dipole matrix in Equation 2.61 turn out to be zero, however this does not imply that the transition is not permitted.

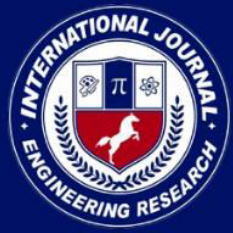
The probability of a forbidden line is determined by the interaction between the electron's magnetic moment and the electromagnetic field (spin-orbit interaction), and in the second order approximation, the magnetic dipole approximation, the probability of a forbidden line is non-zero and is proportional to $M_{if} = i|L + 2S|f$, where M_{if} contains the elements of the magnetic dipole matrix. Analytical criteria for magnetic dipole transitions may be derived for hydrogen-like atoms with a suitable basis.

CONCLUSION

The potential that the ionizing radiation may not reach the ISM near the source is ignored in the assumption that the detection of ionized nebulae would assist us to discover occluded SSS that cannot be identified using X-rays. Attempts to explain the gap between the observed and predicted number of SSSs in galaxies have taken this into account. The circumbinary stellar medium (CSM) surrounding an SSS should be able to mask most of the radiation due to the impact of massive mass loss from the system through a thick wind, as postulated by Nielsen, Dominik, Nelemans, and Voss (2013). Claiming that these hypothetical nebulae would require mass loss rates comparable to the stable-burning accretion rate (10^{-7} to $10^{-6} M_{\odot}$) for a typical SSS system, Nielsen & Gilfanov (2015) used CLOUDY to show that they would look very different from the expected SSS nebulae. Because of the large quantities of CSM material predicted by this scenario, unusual characteristics would be imprinted in the early spectra of an SN Ia. These things have yet to be found.

REFERENCES

1. Callanan, P. J., Machin, G., Naylor, T. & Charles, P. A. 1989, MNRAS, 241, 27p.
2. Carroll, B. W. & Ostlie, D. A. 2007, An Introduction to Modern Astrophysics, 2nd Ed., Pearson Education, Inc.
3. Charles, P. A., Southwell, K. A., & O'Donoghue, D. 1996, IAU Circ, 6305, 2
4. Chandrasekhar S. 1983, On Stars, their Evolution and their stability, Nobel Prize lecture
5. Chen, H.-L., Woods, T. E., Yungelson, L. R., Gilfanov, M., & Han, Z. 2014, MNRAS, 445, 1912
6. Chen H.-L., Woods T. E., Yungelson L. R., Gilfanov M., Han Z., 2015, MNRAS, 453, 3024
7. Chevalier, R. A., Kirshner, R. P., & Raymond, J. C. 1980, ApJ, 235, 186 Chiang, E. & Rappaport, S. 1996, ApJ, 469, 255
8. Choudhury, S., Subramaniam, A., & Cole, A. A. 2016, MNRAS, 455, 1855 Collins, G. W. 1989, New York, W. H. Freeman and Co., 1989, 512 p.
9. Cowperthwaite, P. S., Berger, E., Soares-Santos, M., et al. 2016, ApJ, 826, L29 Covington, A. et al., 2001, Phys. Rev. Lett. 87, 243002
10. Cowley, A. P., Schmidtke, P. C., Crampton, D., & Hutchings, J. B. 1990, ApJ, 350, 288
11. Cowley, A. P., Schmidtke, P. C., Hutchings, J. B., Crampton, D., & McGrath, T. K. 1993, ApJ, 418, L63



12. Crampton, D., Hutchings, J. B., Cowley, A. P., et al. 1996, ApJ, 456, 320 Cumming, R. J., Lundqvist, P., Smith, L. J., Pettini, M., & King, D. L. 1996, MNRAS, 283, 1355